Stability, Oscillatory Modes, Bifurcations, and Chaotic Behavior of Complex Systems with Phase Control

Valerie P. Ponomarenko[1], Nikolay I. Zaytsev[2]

[1, 2]Research Institute of Applied Mathematics and Cybernetics,

Nizhegorodsky State University After N.I. Lobachevski, Nizhni Novgorod, Russia

[1]povp@uic.nnov.ru; [2]nikozay@yandex.ru

***Abstract*-This paper deals with the problem of nonlinear dynamics of complex system with phase control combining phase-locked loop and automatic gain control loop. The behavior of the examined system is described by nonlinear two- and four-dimensional sets of differential equations with periodical nonlinearities. Stability of synchronous mode, bifurcations determining boundaries of domain with quality different behavior of the considered system, and oscillatory modes arising in domain where synchronous mode is unstable are studied. Results are presented using two-parameter bifurcation diagrams, phase portraits of attractors, time realizations of oscillations, and Poincare maps.**

Keywords-Systems with Phase and Gain Control; Nonlinear Dynamics; Stability; Bifurcation; Transitions to Chaos

I. INTRODUCTION

At present, the systems with phase control are widely used. As known [Shakhgil'dyan and Lyakhovkin, 1972; Lindsey, 1972], such systems are traditionally intended to provide for and maintain the synchronous state, when the phase difference of reference and controlled signals becomes constant or, equivalently, the frequency difference of these signals is equal to zero. The systems may be also operating in non-synchronous modes with variable phase and frequency errors. The use of such modes opens wide possibilities for some nontraditional engineering and technological applications of phase control systems (generation of complex periodic and chaotic signals, data transmission and processing, etc. [Dmitriev and Shirokov, 2004; Dmitriev, Kletsov and Kuzmin, 2009]).

Among the studies of the systems with phase control, the study of dynamical modes, bifurcation, and transitions to chaotic behavior is extremely interesting. In this paper we investigate dynamical behavior of complex system with phase control combining phase-locked loop (PLL) and automatic gain control loop (AGCL). Different versions of such systems are of interest because they represent a circuit implementation of optimal algorithms for tracking estimation of variable parameters (phase angle $\vartheta(t)$ and amplitude $A(t)$ of receiving signal [Tikhonov and Kulman, 1975; Kulman, Zheronkina, 1969]).

Combined PLL and AGCL operate on the basic of synchronization between receiving (estimated) and reference signals. For that, PLL performs coincidence of the signals frequencies, and AGCL regulates amplification factor in the phase control loop so as to reduce the influence of input signal amplitude alternation on PLL operation. This paper is mainly devoted to investigation of the characteristics of the system's dynamical behavior that are due to application of first- and second-order low-frequency filters (LFFs) in control circuits, and to coupling via phase and gain control circuits.

II. THE SYSTEM MODELS UNDER CONSIDERATION

Equations describing the dynamics of the considered combined PLL and AGCL can be derived from the equations for estimates ϑ^* and A^* of input signal parameters ϑ and A obtained in [Tikhonov and Kulman, 1975; Kulman, Zheronkina, 1969]. These equations can be represented for mismatch $\varphi=\vartheta(t)-\vartheta^*(t)$ and amplitude ratio $x=A^*/A$ in the operator form ($p\equiv d/dt$) as follows [Ponomarenko, 1986]

$$\left.\begin{aligned} p\varphi/k_1 &= \gamma - K_1(p)\, x \sin\varphi, \\ x &= K_2(p)\left[G_0(x) + k_2\left(\cos\varphi + \alpha x \sin\varphi\right)\right]. \end{aligned}\right\} \quad (1)$$

In Equation (1), k_1 and k_2 are the amplification factors of control circuits; γ is the initial frequency mismatch; $G_0(x)$ depends on the gain control circuit structure and is expressed in the forms of $G_0(x)=\delta_0-k_2x$ and $G_0(x)=\sigma/x-k_2x$ [Tikhonov and Kulman, 1975], $\delta_0=A_0/A$ (A_0 is average input signal amplitude); σ is the gain control circuit parameter; $K_1(p)$ and $K_2(p)$ are the transfer functions of the LLFs in the PLL and AGCL control circuits; and α is the factor of coupling via control circuits. By complexity of Equations (1), we consider amplitude A as constant parameter having arbitrary positive values.

The types of LFFs are determined by the models using for description of dynamics of parameters ϑ and A. Consider the simplest first-order filters with transfer functions $K_1(p)=1$, $K_2(p)=1/(1+T_0p)$, where T_0 is a time constant. Equation (1) may be written in this case as

$$\left.\begin{aligned} d\varphi/d\tau &= \gamma - x\sin\varphi, \\ dx/d\tau &= \lambda\left(G(x) + \cos\varphi + \alpha x \sin\varphi\right), \end{aligned}\right\} \quad (2)$$

where $\tau=k_1t$ is dimensionless time, $G(x)$ is represented by functions: $G(x)=\delta-\beta x$ and $G(x)=\sigma/x-\beta x$, $\beta=1+1/k_2$, $\delta=\delta_0/k_2$, $\lambda=k_2/(T_0k_1)$. System (2) is a dynamical system determined on cylindrical phase surface $U_0=\{\varphi(\mathrm{mod}2\pi),x\}$.

Now consider the second-order filter in the PLL and first-order filter in the AGCL with transfer functions $K_1(p)=1/[1+(T_1+T_2)p+T_1T_2p^2]$, $K_2(p)=1/(1+T_0p)$, where T_1 and T_2 are the time constants. In this case, equation (1) are written as

$$\left.\begin{aligned} &d\varphi/d\tau = y, \quad dy/d\tau = z,\\ &\mu\, dz/d\tau = \gamma - x\sin\varphi - y - \varepsilon_1 z,\\ &\varepsilon_2\, dx/d\tau = G(x) + \cos\varphi + \alpha x\sin\varphi, \end{aligned}\right\} \qquad (3)$$

where $\varepsilon_1=(T_1+T_2)k_1$, $\varepsilon_2=T_0k_1/k_2$, $\mu=T_1T_2k_1^2$. System (3) is a dynamical system with four-dimensional cylindrical phase space $U=\{\varphi(\mathrm{mod}2\pi),y,z,x\}$.

Further, we will consider the Models (2) and (3) for the values of variable $x>0$. Since Models (2) and (3) are nonlinear, its nonlocal study encounters serious difficulties. Therefore, we apply qualitative-numerical methods of nonlinear dynamics and computer simulation.

III. DYNAMICAL STATES OF MODEL

At first, we discuss the problem of local stability of synchronous mode. The equilibrium states of System (2) situated in the half phase cylinder $x>0$ are determined from the equations

$$\gamma - x\sin\varphi = 0,\ G(x) + \cos\varphi + \alpha x\sin\varphi = 0. \qquad (4)$$

Consider Equations (4) as function $G(x)=\delta-\beta x$. In this case, from Equations (4) and the form of G(x), it follows that, for $0<\alpha<\beta$ and the values of $\gamma,\delta,\beta,\alpha\in Co$ where $Co=\{\gamma_1(\delta,\beta,\alpha)<\gamma<\gamma_2(\delta,\beta,\alpha)\}$, system (2) has two equilibrium states $A_1(\varphi_1,x_1)$ and $A_2(\varphi_2,x_2)$. The coordinates φ_1, x_1, φ_2, and x_2 are defined from Equation (4). For $\alpha>\beta$, the domain $Co=\{\gamma>\gamma_1(\delta,\beta,\alpha)\}$. If $\alpha=0$, the boundaries of domain C_0

$$\left.\begin{aligned} &\gamma_1(\delta,\beta) = -\frac{(\sqrt{\delta^2+8}+3\delta)\sqrt{16-(\sqrt{\delta^2+8}-\delta)^2}}{16\beta}\\ &\gamma_2(\delta,\beta) = -\gamma_1(\delta,\beta). \end{aligned}\right\} \qquad (5)$$

Bifurcation values $\gamma=\gamma_1$ and $\gamma=\gamma_2$ corresponding to merging of equilibrium states $A_1(\varphi_1,x_1)$, and $A_2(\varphi_2,x_2)$ are defined from equality

$$\gamma_i(\delta,\beta,\alpha)=\sin\varphi_{m2}(\delta+\cos\varphi_{m2})/(\beta-\alpha\sin\varphi_{m2}),\quad i=1,2. \qquad (6)$$

In Equality (6) $\varphi m2$ is the solution of the equation

$$\beta\cos\varphi(\delta+\cos\varphi)-\sin^3\varphi(\beta-\alpha\sin\varphi)=0. \qquad (7)$$

The values of $\varphi m2$ are satisfied following conditions: $-\pi/2<\varphi m1<0$, $0<\varphi m2<\pi/2$. Fig. 1 shows qualitative disposition of bifurcation curves γ_1 and γ_2, and domain Co on the (γ,δ) plane for $0<\alpha<\beta$ (Fig. 1a) and $\alpha>\beta$ (Fig. 1b).

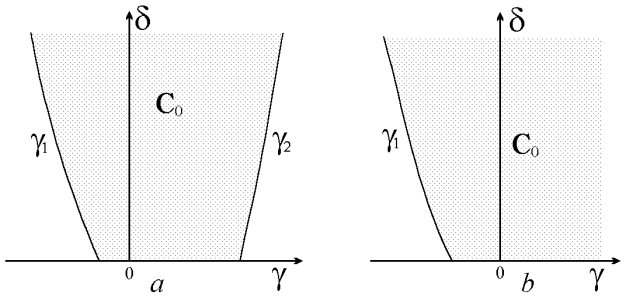

Fig. 1 Disposition of the domain C_0: *a* – $0<\alpha<\beta$, *b* – $\alpha>\beta$

Now consider Equations (4), if function $G(x)=\sigma/x-\beta x$. From (4) and the form of G(x), it follows that, for $0<\alpha<\beta$ and $\gamma,\delta,\beta,\alpha\in D_0$, where $D_0=\{\sigma>\max(\sigma-(\gamma,\beta,\alpha),0,\ \sigma^+(\gamma,\beta,\alpha))\}$, System (2) has also two equilibrium states $A1(\varphi_1,x_1)$ and $A1(\varphi_2,x_2)$. For $\alpha>\beta$, the domain is $D_0=\{\sigma>\max(\sigma-(\gamma,\beta,\alpha),0)\}$. If parameter $\alpha=0$, $\sigma^+(\gamma,\beta,\alpha)=\sigma-(-\gamma,\beta,\alpha)$. Bifurcation values $\sigma=\sigma-$ and $\sigma=\sigma^+$ corresponding to merging of equilibrium states $A_1(\varphi_1,x_1)$ and $A_2(\varphi_2,x_2)$ are defined by

$$\left.\begin{aligned} \sigma^+ &= \frac{\gamma^2(\beta-\alpha\sin\varphi_m^+)-\gamma\sin\varphi_m^+\cos\varphi_m^+}{\sin^2\varphi_m^+},\\ \sigma^- &= \frac{\gamma^2(\beta-\alpha\sin\varphi_m^-)-\gamma\sin\varphi_m^-\cos\varphi_m^-}{\sin^2\varphi_m^-}. \end{aligned}\right\} \qquad (8)$$

In (8) φ_m^+ and φ_m^- ($\varphi_m^+\in(0,\pi/2)$, $\varphi_m^-\in(-\pi/2,0)$) are the solutions of the equation

$$\gamma\,(2\beta-\alpha\sin\varphi)\cos\varphi-\sin\varphi=0. \qquad (9)$$

Disposition of bifurcation curves $\sigma=\sigma-$ and $\sigma=\sigma+$, and domain D_0 on the (γ,σ) plane is qualitatively similar to disposition of curves $\gamma=\gamma_1$ and $\gamma=\gamma_2$ on the (γ,δ) plane given in Fig. 1.

The characteristic equation for system (2) is

$$\chi^2 + q\chi + r = 0. \qquad (10)$$

In (10), if function G(x) takes the form $G(x)=\delta-\beta x$, then

$$\left.\begin{aligned} q &= \lambda(\beta-\alpha\sin\varphi_{1,2}) + x_{1,2}\cos\varphi_{1,2},\\ r &= \lambda(x_{1,2}\cos\varphi_{1,2}(\beta-\alpha\sin\varphi_{1,2}) +\\ &\quad +(\alpha x_{1,2}\cos\varphi_{1,2}-\sin\varphi_{1,2})-\sin\varphi_{1,2}). \end{aligned}\right\} \qquad (11)$$

If function G(x) takes the form $G(x)=\sigma/x-\beta x$, then in Equation (10)

$$\left.\begin{aligned} q &= \lambda(\sigma/x_{1,2}^2+\beta-\alpha\sin\varphi_{1,2})+x_{1,2}\cos\varphi_{1,2},\\ r &= \lambda(x_{1,2}\cos\varphi_{1,2}(\sigma/x_{1,2}^2+\beta-\alpha\sin\varphi_{1,2})-\\ &\quad -\sin\varphi_{1,2}(\sin\varphi_{1,2}-\alpha x_{1,2}\cos\varphi_{1,2})). \end{aligned}\right\} \qquad (12)$$

By investigating the roots of the characteristic Equation (10), we find that the equilibrium state $A_1(\varphi_1,x_1)$ are stable, whereas the equilibrium state $A_2(\varphi_2,x_2)$ is unstable of saddle type.

The equilibrium state A_1 corresponds to synchronous mode of combined PPL and AGCL. If this mode is realized in this system, then the system can carry out tracking of estimated input signal's parameters. The parameter region where such mode exists is limited by the values of parameters γ, δ, β, α, and σ those belong to domains C_0 and D_0. Values φ_1 and x_1 characterize the accuracy with which the parameters of input signal are estimated.

Further, we consider nonlocal dynamic processes evolving in Model (2) when parameters γ, δ, and σ vary and remaining parameters are fixed. The results of qualitative-numerical investigation of Model (2) for $G(x)=\delta-\beta x$ and for $G(x)=\sigma/x-\beta x$ reveal qualitatively similar dynamical states, bifurcation, parametrical portraits on the (γ,δ) plane and (γ,σ) plane, and corresponding phase portraits. Fig. 2 shows qualitative disposition of bifurcation curves on the (γ,δ) plane within the domain Co obtained for System (2), if function G(x) takes the form $G(x)=\delta-\beta x$ and $0<\alpha<\beta$.

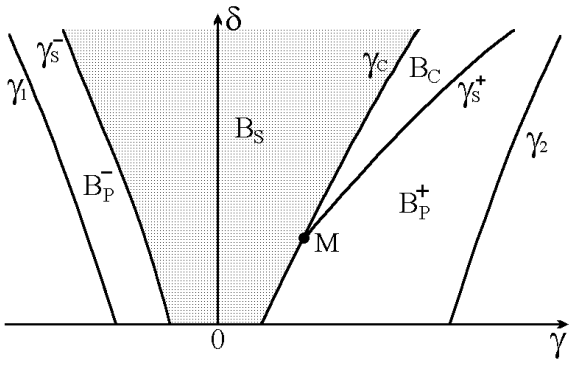

Fig. 2 Bifurcation curve and domains

of dynamical modes

In Fig. 2 lines γ_s^- and γ_s^+ correspond to saddle A_2 separatrix S_1 and S_2 loop Π0 of rotatory type that encompasses the phase cylinder U0. By investigating of saddle value:

$$\sigma_s = -x_2(\gamma,\delta,\beta,\alpha)\cos\varphi_2(\gamma,\delta,\beta,\alpha) - \lambda\beta + \\ + \mu\alpha\sin\varphi_2(\gamma,\delta,\beta,\alpha), \qquad (13)$$

we find that the loop Π0, that arises at $\gamma=\gamma_s^-$, is stable (saddle value σs<0), whereas the loop Π0, that forms at $\gamma=\gamma_s^+$, is stable at the part of the curve γ_s^+ below the point M (where σs<0) and unstable at the part of the curve γ_s^+ above the point M (where σs>0). The point M corresponds to δ=δs(γ, β, α, λ), that defined from the equation σs(γ,δ,β,α,λ)=0.

Therefore, upon passing throw the curve γ_s^-, if γ is decreased, a stable rotatory type (2π-periodic in φ) limit cycle L0 appears in the half phase cylinder x>0. When, as the result of γ increasing, the System (2) crosses line γ_s^+ and δ<δs, a stable rotatory type limit cycle L0 also appears in the half phase cylinder x>0. Upon passing throw the curve γ_s^+, as γ is decreased and δ>δs, an unstable rotatory type limit cycle Γ0 appears in the half phase cylinder x>0.

Line γc starting from the point M corresponds to double rotatory type limit cycle in the half phase cylinder x>0. If, as the result of increasing γ, line γc is crossed, a stable rotational type limit cycle L0 and an unstable rotatory type limit cycle Γ0 are born in the half phase cylinder x>0. Upon passing through the line γc, as γ is decreased, limit cycles L0 and Γ0 merge and disappear.

Limit cycle L0 is associated with the asynchronous mode of the combined PLL and AGCL such that phase error φ rotates and amplitude ratio x periodically oscillate about certain mean value.

Bifurcation curves γ_1, γ_s^-, γ_s^+, γc, and γ2 given at Fig. 2 identify various parameter domains possessing qualitatively different dynamics of the Model (2). Fig. 3 shows the phase portraits of the System (2) for dynamic mode domains represented in Fig. 2. For the parameters from domain $B_S=\{\gamma_s^- < \gamma < \min(\gamma_s^+, \gamma c)\}$ there are no limit cycles and equilibrium state A_1 of System (2) is globally asymptotically stable in the half phase cylinder x>0. The phase trajectories of System (2) converge to A_1 independently of initial state of the system (Fig.3a). Therefore, when the values of the system parameters belong to domain Bs, the combined PLL and AGCL is in synchronous mode irrespective of the initial conditions.

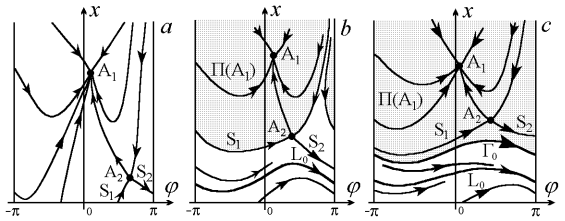

Fig. 3 Phase portraits of model (2)

For the parameters from domains $B_p^- = \{\gamma_1 < \gamma < \gamma_s^-\}$ and $B_p^+ = \{\gamma_s^+ < \gamma < \gamma 2\}$ a stable equilibrium state A_1 and stable limit cycle L0 are simultaneously exist on the phase cylinder U0 (Fig. 3b). Depending on initial state, the trajectories of System (2) converge either to equilibrium state A_1 or to limit cycle L0. Therefore, depending on initial conditions, synchronous or asynchronous mode corresponding to these attractors on the phase cylinder U0 develops in the combined PLL and AGCL. The regions of attraction of equilibrium state A_1 and limit cycles L0 are bounded by of saddle A_2 separatrix on the phase cylinder U0. For the parameters from domain $Bc=\{\gamma c < \gamma < \gamma_s^+\}$ there are equilibrium state A_1 and limit cycles L0 and Γ0 on the phase cylinder U0 (Fig. 3c). The region Π(A1) of attraction of equilibrium state A_1 is bounded by unstable limit cycle Γ0. Therefore, if the initial conditions belong to domain located above limit cycle Γ0, then the synchronous mode is realized in combined PLL and AGCL.

From the results obtained in framework of Model (2) we infer that, coupling via feedback signals in combined PLL and AGCL with the first-order filters make possible the appearance of asynchronous mode of rotational limit cycle, which is not possible in partial PLL and AGCL.

IV. PECULIARITIES OF MODEL (3) DYNAMICAL BEHAVIOR

If second-order LFF is used in the PLL, the dynamics of combined PLL and AGCL becomes drastically more complex. In addition to the synchronous mode and the periodic asynchronous mode, complex-periodic and chaotic asynchronous modes appear. Apart from this, the synchronous mode may lose stability and a transition to a periodic quasi-synchronous mode characterized by an oscillatory-type limit cycle may occur, the quasi-synchronous mode may become chaotic. Besides, the system may exhibits quasi-synchronous and asynchronous modes of quasi-periodic types corresponding to oscillatory and rotational two-dimension tori in the phase space.

First, let us analyze the stability of the combined PLL and AGCL synchronous mode. System (3) with parameters $\gamma,\delta,\beta,\alpha \in Co$ and $\gamma,\sigma,\beta,\alpha \in D_0$ has two equilibrium states $A_1(\varphi_1,0,0,x_1)$ and $A_2(\varphi_2,0,0,x_2)$ located within the range x>0 of phase space U; coordinates $\varphi_1, x_1, \varphi_2$, and x_2 are determined from (4). Equilibrium state A_1 may be either stable or unstable, while equilibrium state A_2 is unstable of saddle type.

The conditions under which equilibrium state A_1 is stable are determined by the roots of characteristic

Equation:

$$\chi^4 + a_1\chi^3 + a_2\chi^2 + a_3\chi + a_4 = 0, \qquad (14)$$

where

$$\left.\begin{aligned} a_1 &= \varepsilon_1/\mu - (G'(x_n) + \alpha\sin\varphi_n)/\varepsilon_2, \\ a_2 &= (1 - \varepsilon_1(G'(x_n) + \alpha\sin\varphi_n)/\varepsilon_2)/\mu, \\ a_3 &= (x_n\cos\varphi_n - (G'(x_n) + \alpha\sin\varphi_n)/\varepsilon_2))/\mu, \\ a_4 &= -(\sin^2\varphi_n + x_n G'(x_n)\cos\varphi_n)/(\mu\varepsilon_2). \end{aligned}\right\} \qquad (15)$$

Applying the Routh-Hurwits criterion to the Equation (14), we obtained that equilibrium state A_1 is stable for the values of parameters such that the following inequalities hold:

$$a_1,a_2,a_3,a_4>0,\ a_1a_2-a_3>0,\ a_3(a_1a_2-a_3)-a_1^2a_4>0. \qquad (16)$$

If Condition (16) are satisfied, the combined PLL and AGCL described by Model (3) have a synchronous mode corresponding to equilibrium state $A_1(\varphi_1,0,0,x_1)$.

The domain of parameters Cs0 where Conditions (16) are satisfied corresponds to the region where the synchronous mode persists. Figs. 4 and 5 show boundary of the domains Co and D_0 where the equilibrium states exist (curve γ_1) and boundary of domain Cs0 where equilibrium state A_1 is stable (curve γs), for $G(x)=\delta-\beta x$ (Fig. 4) and $G(x)=\sigma/x-\beta x$ (Fig. 5) correspondently.

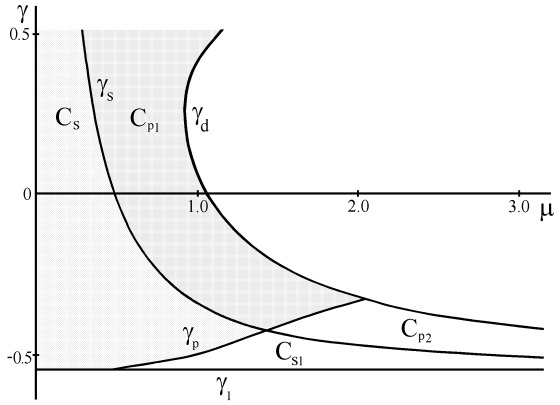

Fig. 4 Bifurcation diagram (μ,γ) for G(x)=δ−βx

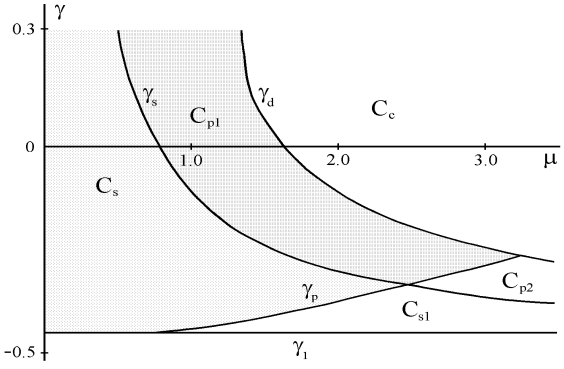

Fig. 5 Bifurcation diagram (μ,γ) for G(x)=σ/x−βx

The curves γ_1 and γs, and other bifurcation curves are plotted on plane (μ,γ) for the values of parameters α=2, β=1.1, ε_1=1, ε_2=2, δ=1.25, σ=0.5. The domain Cs0 is located between the lines γs and γ_1.

The domain Cs0 is divided by the curve γp into domains Cs: {max (γ_1,γp)<γ<γs} and Cs_1:{γ_1<γ<min(γp, γs)}. The curve γp corresponds to the bifurcation of saddle-focus A_2 separatrix loop rotatory type (Re$\chi_{1,2}$<0, Im$\chi_{1,2}\neq$0, χ_3<0, χ_4>0, where χ1,2,3,4 are the roots of the characteristic equation (14) for the equilibrium state A_2). For the parameters from domain C_s, the equilibrium state A_1 is only attractor in the phase space U. The trajectories in the phase space converge to A_1 independently of initial state of the system. Therefore, the domain C_s is a locking region of the combined PLL and AGCL. When the values of the Model (3) parameters belong to domain C_s, the system is in the synchronous mode irrespective of the initial conditions.

Now let us consider qualitative change of the system's behavior that occurs owing to variations in γ and μ during the exit from domain C_s. When, as a result of growing γ or μ, the system crosses boundary γs, Conditions (16) are violated and System (3) exhibits the Andronov-Hopf supercritical bifurcation. The latter is related to a solution to characteristic Equation (14) containing a pair of complex-conjugated roots with a positive real part. At the same time, oscillatory type limit cycle S1 such that phase difference φ varies within a limited range not exceeding 2π appears in phase space U. Cycle S1 corresponds to a quasi-synchronous mode in the combined PLL and AGCL where periodic oscillations of phase variables are observed around equilibrium state A_1 that has become unstable. Fig. 6a shows (φ,y)-projection of phase portrait and time waveform y(τ) corresponding to the mode of cycle S1 of model (3) for $G(x)=\delta-\beta x$.

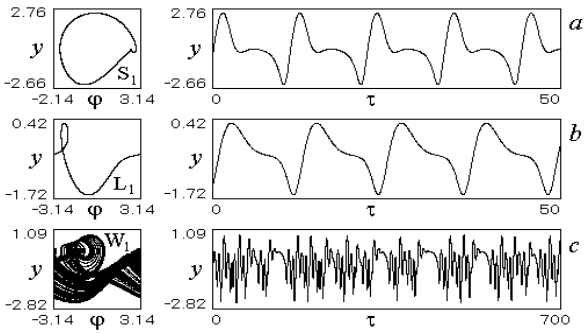

Fig. 6 Nonsynchronous modes of model (3) for $G(x)=\delta-\beta x$ and γ=0.86, μ=0.727 (a); γ=−0.54, μ=1.6 (b), 2.63 (c) (α=2, β=1.1, δ=1.25, ε_1=1, ε_2=2)

If, as a result of increasing μ or decreasing γ, the system crosses line γp (where the saddle value $\sigma p=\chi_4+\mathrm{Re}\chi m<0$, m=1,2,3) a stable rotatory type limit cycle L1 appears in the phase space U. In the mode of limit cycle L1 phase difference φ rotates and variables y,z, and x periodically oscillate about certain mean values.

Upon changing of parameters γ and μ within the domain C_{s1} (see Figs. 4, 5) limit cycle L1 may disappear in the result of saddle-node bifurcation. After this bifurcation, the system undergoes a transition to the mode of rotatory chaotic attractor W_1 via intermittence. Figs.6b, 6c show examples of (φ,y)-projections of phase portraits and dependences y(τ) corresponding to the modes of attractors L_1 and W_1 of Model (3) for $G(x)=\delta-\beta x$. Modeling of System (3) indicates that complex multi turn-over rotatory type limit cycles exist in the phase space U when the system's parameters belong to domain C_{s1}. Therefore, in domain C_{s1}, combined PLL and AGCL have concurrent synchronous mode and asynchronous mode determined by stable equilibrium state and periodic or chaotic attractors of rotatory type. The initial conditions determine

which of these modes is realized in the system for parameters from the domain C_{s1}.

The quasi-synchronous mode of limit cycle S1 exists for the values of parameters belonging to domain Cp_0 restricted by the curves γs and γd (see Figs. 4, 5). Curve γd corresponds to the loss of stability of limit cycle S1 as the result of the period-doubling bifurcation. The domain Cp_0 is divided by bifurcation curve γp into domain Cp_1: {max(γs,γp)<γ<γd} and Cp_2: {γs<γ<min(γp, γd)}. For the parameter values from domain Cp_1, limit cycle S1 is globally stable. While for the parameters from domain Cp_2 -the Model (3) exhibits bistable behavior, the limit cycle S1 and periodic or chaotic modes of attractors of rotational type concurrently exist in the phase space U. Transitions to the chaotic mode are realized via period-doubling bifurcations of rotatory limit cycles and so via intermittence.

In domain C_c, located to the right of line γd, the Model (3) exhibits complex dynamical behavior. For parameters from the domain C_c quasi-synchronous and asynchronous modes of various complexities are realized in the combined PLL and AGCL.

Let us track the evolution of the mode of limit cycle S1 when parameter μ is increased. For this purpose, we use the results of numerical simulation of Model (3) for $G(x)=\sigma/x-\beta x$. The non-synchronous modes formed when parameter μ varies are illustrated by one-parameter bifurcation {μ,y} diagram of the Poincare mapping corresponding to σ=0.5, β=1.1, α=2, ε_1=1, ε_2=2, γ=0.1, and μ∈(1.4;2.82) (Fig.7), (φ,y) projections of the attractors' phase portraits, and fragments of dependences y(τ) (Fig.8).

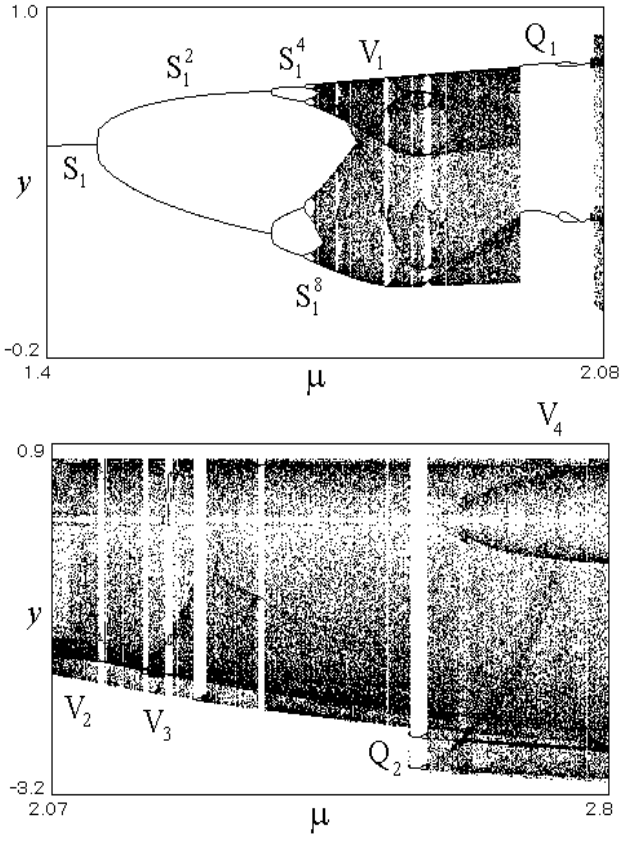

Fig. 7 Diagram showing evolution of quasi-synchronous mode of limit cycle S_1 during variation of μ for $G(x)=\sigma/x-\beta x$

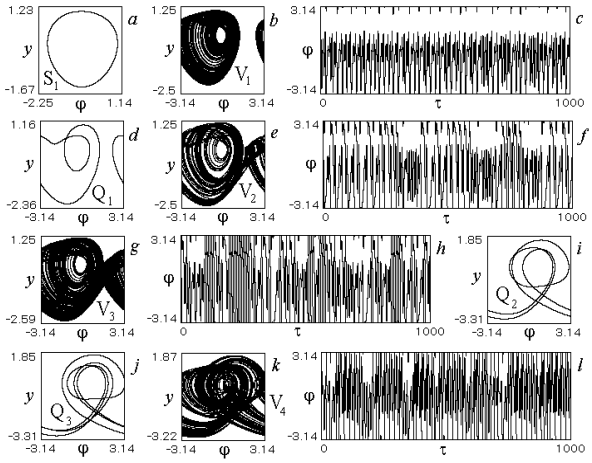

Fig. 8 Projections of phase portraits and fragments of time-realizations of oscillations corresponding to attractors of model (3) for $G(x)=\sigma/x-\beta x$, μ=1.4 (a); 1.95 (b,c); 2.0 (d);

2.07 (e,f); 2.21 (g,h); 2.55 (i); 2.62 (j); 2.82 (k,l)

(σ=0.5, β=1.1, α=2, ε_1=1, ε_2=2, γ=0.1)

The quasi-synchronous mode of limit cycle S1 is the system's initial state. When μ increases, cycle S1 exhibits period-doubling bifurcations, which finally end in a transition to the mode of oscillatory chaotic attractor V_1 (Figs. 8b, c). After that, the oscillations in the mode of attractor V_1 transform rigidly into the oscillations in the mode of oscillatory limit cycle Q_1 (Fig. 8d). When μ>2.07, the system switches from the mode of limit cycle Q_1 to the mode of chaotic attractor V_2 of oscillatory-rotatory type (Figs. 8e,f). Then, alternating chaotic and periodic asynchronous modes are observed; in the majority of the studied μ range, chaotic modes are realized. Examples of phase portraits and time realization y(τ) of chaotic and periodic modes are shown in Figs. 8g-8l.

Numerical simulation of Model (3) reveals that this model may demonstrate such interesting dynamical phenomena as formation of attracting two-dimensional tori of oscillatory and rotatory types in the phase space U. These tori appear as the result of loss of oscillatory or rotatory limit cycles stability when a pair of complex-conjugated cycles, multiplicators crosses a unit circle. The tori correspond to two-frequency non-synchronous modes of combined PLL and AGCL.

Fig. 9 illustrates the examples of the (φ,x)-projection of phase portraits, dependences x(τ), and (y, x)-projections of Poincare mapping T generated by the phase trajectories of Model (3) corresponding to $G(x)=\delta-\beta x$ and β=1.1, δ=1.25, γ=0.1, μ=5, ε_1=1.97, ε_2=150. The results represented in Fig. 9 characterize non-synchronous modes of the system formed when coupling parameter α varies. The quasi-synchronous mode of limit cycle S_2 (see Fig. 9a) is the system's starting state for α=1.6.

When α increases, the mode of oscillatory torus T1 (Fig. 9b) appears from limit cycle S_2. The phase portrait of mapping T (Fig. 9c) is characterized by the presence of stable closed invariant curve Γ_1. When 1.623<μ<1.92, the alternation of the mode of torus T1 and the modes of multi turn-over limit cycles of oscillatory type are observed. An example of nine-turn limit cycle S_3 is represented in Fig. 9d. Beginning with α=1.92, the distortion of the curve Γ_1 is observed. This phenomenon indicates gradual transformation the mode of torus T1 to the mode of oscillatory type chaotic attractor P_1 (Fig. 9e).

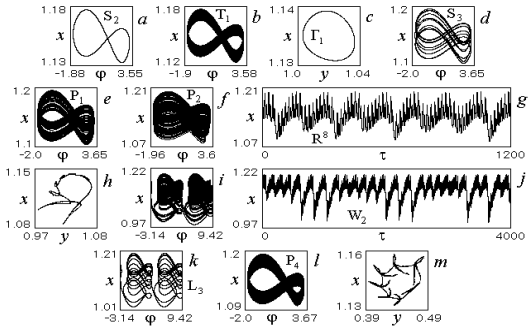

Fig. 9 Attractors of model (3) for G(x)=δ−βx and

α=1.6 (a); 1.65 (b,c); 1.9 (d); 1.946 (e); 2.08 (f,g,h);

2.097 (i,j); 2.35 (k); 2.436 (l,m)

(γ=0.1, μ=5, β=1.1, δ=1.25, ε1=1.97, ε2=150)

As α further increases, rigid transition of the system from the mode of chaotic attractor P_1 to the mode of oscillatory eight-turn limit cycle S_4 take place. With further increase of α the mode of cycle S_4 is transformed to the mode of chaotic attractor P_2 (Fig. 9f,g,h). Upon reaching the value α=2.088, rotatory phase trajectory scrolls in the attractor's P_2 structure are appeared. This phenomenon indicates transformation the mode of oscillatory attractor P_2 to the mode of oscillatory-rotatory chaotic attractor W_2 (Fig. 9i, j). A still increase of α leads to the alternation of the modes of complex limit cycles of oscillatory-rotatory types (Fig. 9k) and the modes of chaotic attractors (Fig. 9l, m) and following returning to the mode of periodic quasi-synchronous mode.

The existence of rotatory tori in phase space U is revealed in the model (3) for G(x)=δ−βx and β=1.1, δ=1.25, α=5, μ=5, ε_1=1, ε_2=150 when parameter γ is varied. Figure 10 displaying the examples of (φ,y)-projection of phase portraits, dependences y(τ), and (y,x)-projections of Poincare mapping Tφ of the plane φ=φ_0 into the plane φ=φ_0+2π produced by the trajectories of model (3) shows how mismatch γ affects the process of the asynchronous mode of limit cycle L_2 (Fig. 10a) transformation during a decrease in γ.

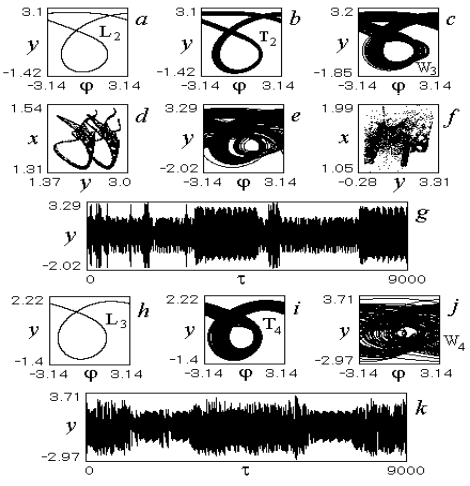

Fig. 10 Attractors of model (3) for G(x)=δ−βx and

γ=0.853 (a); 0.845 (b); 0.819 (c,d); 0.818 (e,f,g);

0.362 (h); 0.323 (i); 0.32 (j,k)

(α=5, μ=5, β=1.1, δ=1.25, ε_1=1.0, ε_2=150)

At first, the mode of limit cycle L_2 is transformed to the mode of rotatory torus T2 (Fig. 10b). Torus T2 corresponds to asynchronous two-frequency mode of the combined PLL and AGCL. Further, the following phenomena are observed in the system with decreasing γ: alternation of the mode of torus T2 and the modes of asynchronous modes of multi turn-over rotatory limit cycles; gradual transformation of torus T2 to chaotic attractor W3 (Fig. 10c, d); alternation of chaotic (Fig. 10e, f, g) and periodic modes, the latter of which is determined by two-, four-, and three-turn rotatory limit cycles; soft transformation of the mode of three-turn rotatory limit cycle to the mode of rotatory torus T3; distortion of the torus T3 and following transition to the chaotic mode. A still decrease of γ leads to transition of the system to the asynchronous mode of rotatory limit cycle L_3 (Fig. 10h) and following soft transformation of mode of cycle L_3 to the mode of rotatory torus T4 (Fig. 10i). When γ continues to decrease, the mode of torus T4 is transformed to the mode of rotatory chaotic attractor W_4 (Fig. 10j, k).

V. CONCLUSION

In this paper, we have investigated the dynamical modes, bifurcation, and transitions to the chaotic behavior in a combined PLL and AGCL with the first- and second-order filters in PLL and the first-order filter in AGCL. Using the dynamical models of considered systems, we found that the systems exhibit a rich variety of dynamical modes including synchronous mode, periodic quasi-synchronous mode caused by the loss of the synchronous mode stability, asynchronous modes of rotatory and oscillatory-rotatory limit cycles, quasi-periodic quasi-synchronous and asynchronous modes corresponding to oscillatory and rotatory 2D tori in the phase space, chaotic modes that formed via period-doubling bifurcations, via intermittence, as well as rigidly formed through saddle-node bifurcations of limit cycles, via destruction of tori. These phenomena, in our opinion, are of importance for both basic and applied research of nonlinear dynamics of complex systems with phase control. It allows describing and explaining the behavior of the system when the synchronous state is cut off as a result of the system parameters perturbation. The wide variety of chaotic modes offers considerable possibilities of forming various frequency- and amplitude-modulated signals at the output of the system. Control the characteristics of generated signals can be easily realized by means of system's parameters.

REFERENCES

[1] Shakhgil'dyan, V. V. and Lyakhovkin, A. A. (1972). Phase-Lock Systems. Svyaz', Moscow [in Russian].

[2] Lindsey W. (1972). Synchronization Systems in Communication and Control, Prentice-Hall, Englewood Cliffs, New Jersey.

[3] Dnitriev, A.S. and Shirokov, M.E. (2004). Choice of oscillator for direct chaotic communication system. Radiotekh. Electron. (Moscow), 49 (7), pp. 840-849. [in Russian].

[4] Dnitriev, A.S., Kletsov, A.V., and Kuzmin, K.V. (2009). Generation of ultra wideband phase chaos in decimeter range. Radiotekh. Electron. (Moscow), 54 (6), pp. 709-718. [in Russian].

[5] Tikhonov, V. I. and Kulman, N.K. (1975). Nonlinear filtering and quasi-coherent of signals reception. Sovetskoe Radio. Moscow [in Russian].

[6] Kulman, N.K. and Zheronkina, N.N. (1969). Optimum reception noise immunity of quasi-harmonic process with mutual correlated amplitude and phase. Radiotekh. Electron. (Moscow), 14 (11), pp. 2050-2054. [in Russian].

[7] Ponomarenko, V.P. (1986). On modes and capture range of phase locked loop with control gain circuit. Radiotekh. Electron. (Moscow), 31 (10), pp. 2023-2031. [in Russian].